



# Modeling shear strength of medium- to ultra-high-strength concrete beams with stirrups using SVR and genetic algorithm

Chun-Song Jiang<sup>1,2</sup> · Gui-Qin Liang<sup>3</sup>

Accepted: 2 July 2021 / Published online: 12 July 2021

© The Author(s), under exclusive licence to Springer-Verlag GmbH Germany, part of Springer Nature 2021

## Abstract

This paper presents a data-driven machine learning approach of support vector regression (SVR) with genetic algorithm (GA) optimization approach called SVR-GA for predicting the shear strength capacity of medium- to ultra-high strength concrete beams with longitudinal reinforcement and vertical stirrups. One hundred and forty eight experimental samples collected with different geometric, material and physical factors from literature were utilized for SVR-GA with fivefold cross validation. Shear influence factors such as the stirrup spacing, the beam width, the shear span-to-depth ratio, the effective depth of the beam, the concrete compressive and tensile strength, the longitudinal reinforcement ratio, the product of stirrup ratio and stirrup yield strength were served as input variables. The simulation results show that SVR-GA model can achieve highest accuracy in shear strength prediction based on testing set with a coefficient of determination ( $R^2$ ) of 0.9642, root mean squared error of 1.4685 and mean absolute error of 1.0216 superior to that for traditional SVR model with 0.9379, 2.0375 and 1.4917, which both perform better than multiple linear regression and ACI-318. Furthermore, the sensitivity analysis reveals the most important variables affecting the result of shear strength prediction are shear span-to-depth ratio, concrete compressive strength, reinforcement ratio and the product of stirrup ratio and stirrup yield strength. Three-dimensional input/output maps are employed to reflect the nonlinear variation of the shear strength with the two coupling variables. All in all, the proposed SVR-GA model can achieve excellent accuracy in prediction the shear strength of medium- to ultra-high strength concrete beams with stirrups in comparison with results obtained by traditional SVR, MLP and ACI-318.

**Keywords** Shear strength · Ultra-high strength concrete beams · Stirrups · Support vector regression · Genetic algorithm

## 1 Introduction

The shear failure of reinforced concrete beams with stirrups is a common concern of structural engineers (Collins et al. 2008; Sagaseta and Vollum 2011; Słowik 2014). However, it is difficult to predict the shear failure accurately due to the influence of a large number of parameters, such as stirrup spacing, width and effective depth of the

beam, shear span-to-depth ratio, stirrup ratio, longitudinal reinforcement ratio, tensile compressive strength of concrete, and stirrup yield strength. This difficulty is particularly evident in ultra-high strength concrete (UHSC) and ultra-high performance concrete (UHPC) beams (Hossain et al. 2017).

In order to accurately estimate the shear capacity of UHPC beams, the shear capacity is artificially divided into concrete shear capacity and stirrup yield shear capacity. An additional shear contribution of steel fiber would be added while adding steel fiber into concrete. Further, an additional shear contribution of the pin would be superimposed when taking the pin action of longitudinal reinforcement into account (Yoo and Yoon 2016; Marì Bernat et al. 2020). However, these factors are not independent of each other, and there is a coupling effect between them. For example, the residual tensile stress between cracks will be

✉ Chun-Song Jiang  
jchs2015@glut.edu.cn

<sup>1</sup> Guangxi Key Laboratory of New Energy and Building Energy Saving, Guilin 541004, Guangxi, China

<sup>2</sup> College of Civil and Architecture Engineering, Guilin University of Technology, Guilin 541004, Guangxi, China

<sup>3</sup> College of Information Science and Engineering, Guilin University of Technology, Guilin 541004, Guangxi, China

increased by appropriately adding the steel fiber while both increasing the shear contribution of the fiber and concrete.

A variety of normative formulas or models are proposed to solve problems in engineering applications. However, there are great differences in selecting main variables affecting the shear strength, such as the code of China for the design of concrete structures (GB 50010-2010, Press 2010) uses the concrete tensile strength to calculate the shear strength, while the American concrete structure design code (ACI 318-14, ACI Committee 318 2014) adopts the concrete compressive strength for that. The tensile strength and compressive strength of concrete are both considered by the Chinese highway and bridge code (JTG 3362-2018, Ministry of Transport of China 2018). Although there is little difference between UHPC and normal concrete in the ratio of tensile strength to compressive strength. The addition of steel fibers has greatly affected the tensile strength of UHPC while almost no influence on the compressive strength (Hassan et al. 2012; Krassowska et al. 2019). It is noteworthy that most of the formulas in the codes have been tested on the limited data which is just an extension of the existing empirical formulas for the shear strength of medium and high strength concrete beams, without fully considering and utilizing the ultra-high mechanical properties of ultra-high strength concrete.

Traditional models/equations with low accuracy mainly rely on basic expressions and step-by-step refinement process, it is urgent to propose more accurate method to calculate the shear strength of UHPC beams. Recently, the data-driven machine learning (ML) methods have attracted extensive attention, because of their inherent ability of overcoming the shortcomings of traditional algorithms by relying on manual design features (Liu et al. 2017). Artificial neural network (Açikgenç et al. 2015; Golafshani et al. 2015; Hossain et al. 2017), adaptive fuzzy neural network (Mansouri et al. 2016; Nguyen et al. 2020), Gaussian process regression (Hoang et al. 2016; Guo and Hesthaven 2018) and support vector machine (Pal and Deswal 2011; Farfani et al. 2015) have been widely applied to model the mechanical properties of concrete structures.

ML model uses samples with input and output for training models that can be used to predict the output of new inputs. At present, ML models have been employed to predict the shear capacity of normal concrete beams or ultra-high strength concrete beams without stirrups (Solhmirzaei et al. 2020; Zhang et al. 2020). However, few studies were found for applying machine learning approach to predict the shear capacity of ultra-high strength concrete beams with stirrups. Support vector machine (SVM) is one of ML methods based on statistical learning theory of structural risk minimization. Also known as maximum interval classifier, it is very popular for solving multi-class

problems by establishing a group of 2-class classifiers or establishing a multi-class classifier (Teng et al. 2018). It is called support vector regression (SVR) for solving regression problems. SVR has the advantages of fast learning, global optimization, avoiding local minimization and excellent generalization ability (Çevik et al. 2015), while it is difficult to determine proper parameters for SVR model (Yu et al. 2006; Ccoicca 2013). GA can not only be used to solve the optimization problem directly (Deveci and Demirel 2016), but also optimize the model parameters (Yan and Lin 2016). Here, GA is introduced to simulate biological evolution process to search globally optimal hyper-parameter for SVR.

The remainder of this paper is organized in the following order. Section 2 introduces the background overview, Sect. 3 shows the data structure including the collected experimental results, Sect. 4 describes the proposed SVR-GA model, Sect. 5 presents the model implementation and performance metrics, Sect. 6 presents a performance comparison of SVR-GA, SVR, MLP and ACI 318, the sensitivity analysis for the input variables and the experimental results and analysis. Finally, Sect. 7 provides the conclusions of this study.

## 2 Literature review

With the wide application of high strength concrete, the shear capacity of high-strength and ultra-high strength reinforced concrete beam is one of the most important calculation problems in the design of reinforced concrete frames. In order to reveal and predict the performance of high strength beam and to find the most important parameters affecting the shear capacity, a number of studies have been carried out in the last 2 decades. Zhang (2005) used the modified compression field theory model to predict the shear capacity of high strength concrete beams. The influence of steel fiber and stirrups on the shear strength of steel fiber high-strength concrete beams was analyzed. The results showed that it is not reasonable for steel fiber to completely replace stirrups to improve the shear capacity of beams. Compared with ordinary concrete beam, high strength concrete beam has higher shear strength and better deformation capacity (Ji et al. 2011), and the shear strength decreases with the increase in the shear span-to-depth ratio while increases with the increase in longitudinal reinforcement ratio and stirrup ratio. For the ultra-high performance fiber reinforced concrete (UHPRC) beam, the stirrup spacing exceeds the spacing limits recommended by the design code of ACI 318, but the test values of shear strength are significantly larger than the calculated values of ACI 318 (Lim and Hong 2016). The stirrup spacing required by ACI 318 for reinforced

concrete beams is not suitable for UHPFRC deep beams (Yousef et al. 2018). The tensile strength of UHPC can be increased when adding a certain amount of steel fiber, but that has little effect on the compressive strength. In addition, steel fiber can enhance the ultimate shear strength of reinforced concrete beams (Krassowska et al. 2019). Based on the concept of piecemeal superposition, Qi et al. (2020) established the theoretical calculation formula for the shear capacity of UHPC beams considering the contribution of concrete, stirrups and fibers. The analysis results show that the formula is in good agreement with the experimental data only containing 11 samples.

Pal and Deswal (2011) established a SVR model to predict the shear strength of prestressed reinforced concrete deep beams. The results showed that SVR model is superior to empirical relationship and back propagation neural network in terms of prediction ability. And the concrete cylinder strength and shear span-to-depth ratio are of great significance to the strength prediction of deep beams. Some researchers used intelligent algorithms to optimize model parameters, such as genetic algorithm (GA) to optimize a portion of the existing method (Zhang et al. 2020), and the results obtained by this method are improved compared to other machine learning methods including classical SVR, ANN and gradient boosted decision trees (GBDTs). Solhmirzaei et al. (2020) presented a data-driven ML framework for the failure mode and shear strength capacity of UHPC beams. The results showed that different ML algorithms SVM, ANN, and K-nearest neighbor (K-NN) were effective to classify the shear, flexure-shear, and flexure failure modes. SVM and K-NN algorithms were better than ANN in identifying shear failure mode and flexure-shear failure modes. The explicit expression proposed by GP can predict the shear capacity of UHPC beams with  $R^2$  of 0.92.

One concern of ML model is that the input data are sparse matrices of high dimensions, which are mostly missing or zero (Luo et al. 2018a). To solve this problem of the automatic web-service selection, making highly accurate predictions for missing quality of service (QoS) data via building an ensemble of non-negative latent factor models (Luo et al. 2016). In order to further generate highly accurate predictions for missing QoS data, the second-order solver into latent factor models are proposed (Luo et al. 2018b). Recently, the momentum-incorporated parallel stochastic gradient descent algorithm has also been applied to solve sparse matrix problems by implementing parallelization and accelerating convergence rate (Luo et al. 2021).

Another main problem of SVR is to choose proper parameters and kernel function, which needs to take time for trial and error (Yu et al. 2006; Ccoicca 2013). One method is to solve the problem of optimal hyper-parameter determination through grid search (Zhang et al. 2018),

which is time-consuming while traversing all grids within the parameter value range. Another efficient way to do this is through genetic algorithm (GA), which has been used as a powerful optimization tool to solve a variety of academic and engineering problems. For example, to solve the airline crew pairing problem, an improved dynamic-based GA has been proposed (Deveci and Demirel 2016, 2018; Demirel and Deveci 2017). To predict the failure of the RC structure, GA are explored the optimal initial weights and biases for ANN with single and multiple objective to avoid falling into local minima (Yan and Lin 2016; Chatterjee et al. 2017; Umeonyiagu and Nwobi-Okoye 2019).

It is concluded ML models can be useful tool in predicting shear capacity of concrete beams, and GA can be an effective method to optimize parameters for ML models, which is introduced to select optimal parameters for SVR. Few studies were conducted to apply ML approach to predict the shear strength of ultra-high strength concrete beams with stirrups due to the complexity of the calculation. Therefore, we proposed a hybrid SVR-GA model to solve this problem.

In this study, a hybrid SVR-GA is proposed to predict the shear strength of medium- to ultra-high-strength strength concrete beams with stirrups. The major contributions are as follows:

- 1) Employment of a ML model combining SVR with GA optimization approach to predict the shear strength of medium- to ultra-high-strength strength concrete beams with stirrups.
- 2) Comparison results of ACI-318 and ML models including SVR-GA, SVR and multiple linear regression (MLR) to obtain the model with highest precision for shear strength prediction.
- 3) Utility of parametric sensitivity analysis with three-dimensional visualization map to reveal the inputs that have significant influence on shear strength prediction.

Our proposed model can provide a guide with high accuracy for the performance analysis and optimal design of the shear strength of medium- to ultra-high strength concrete beams with stirrups.

### 3 Data construction

The experimental dataset in this study was collected from previously published works discussing about the shear strength of the simply supported beam (Zhang 2005; Magureanu et al. 2010; Ji et al. 2011; Baby et al. 2014; Xu et al. 2014; Kamal et al. 2014; Zhou and Chen 2015; Hou et al. 2015; Jin et al. 2015; Lim and Hong 2016; Pansuk et al. 2017; Smarzewski 2018; Yousef et al. 2018; Mészöly and Randl 2018; Hasgul et al. 2019; Zheng et al. 2019;

Krassowska et al. 2019; Qi et al. 2020; Wang et al. 2020). The typical RC beam with stirrups and its geometric parameters are illustrated in Fig. 1. The paper review helped determine the factors affecting the beam’s shear capacity (Russo et al. 2004; Olalusi and Viljoen 2020). Various related factors used to predict ultimate shear capacity ( $V_u$ ) are shown in Table 1, including different geometric, material and physical factors, such as stirrup spacing ( $s$ ), beam width ( $b$ ), shear span-to-depth ratio ( $a/d$ ), effective depth of the beam ( $d$ ), concrete compressive strength ( $f_c$ ), concrete tensile strength ( $f_t$ ), longitudinal reinforcement ratio ( $\rho$ ), as well as the product of the stirrup ratio and the stirrup yield strength ( $\rho_s f_{yv}$ ). In this study, the normalized ultimate shear strength [i.e.,  $v_u = V_u/(bd)$ ] (Zhang et al. 2020) was used as a measure for evaluating the shear resistance of the beam.

### 4 Machine learning methods

#### 4.1 Support vector regression (SVR)

Suppose a sample is represented by  $\{(x_i, y_i), i = 1, 2, \dots, n\}$ , where  $x_i$  and  $y_i$  correspond to its input and output, respectively. In SVR, the fundamental idea is to map  $x_i$  to a high-dimensional feature space  $F$  through a nonlinear mapping function  $\Phi(x_i)$ . The goal of SVR is to perform linear regression in this space and find the following linear equation (Vapnik et al. 1997) defined in Eq. 1.

$$f(x) = w \cdot \Phi(x) + b, \Phi : R^n \rightarrow F, w \in F \tag{1}$$

where  $w$  and  $b$  are the normal vector and scalar, respectively. They can be derived from the minimized regularization risk function (Vapnik et al. 1997) showed in Eq. 2 as follows:

$$\begin{aligned} \min R(\alpha, \alpha^*) &= \sum_{i,j=1}^n (\alpha_i - \alpha_i^*) (\alpha_j - \alpha_j^*) K(x_i, x_j) \\ &+ \sum_{i=1}^n \alpha_i (\varepsilon - y_i) + \sum_{i=1}^n \alpha_i^* (\varepsilon + y_i) \end{aligned} \tag{2}$$

Subject to  $\begin{cases} \sum_{i=1}^n (\alpha_i - \alpha_i^*) = 0 \\ \alpha_i, \alpha_i^* \in [0, C] \end{cases}$

where  $C$  is the positive penalty coefficient, which is the

tradeoff between model training error and model flatness.  $\varepsilon$  is the insensitivity coefficient, which determines the error tolerance.  $\alpha_i$  and  $\alpha_i^*$  are the Lagrange multipliers related to the constraint.  $K(x, x_i) = \Phi(x) \cdot \Phi(x_i)$  is the kernel function. After determining  $\alpha_i, \alpha_i^*$  and  $b$  the linear function in Eq. 1 can be expressed explicitly by Eq. 3.

$$f(x) = \sum_{i=1}^n (\alpha_i - \alpha_i^*) K(x, x_i) + b \tag{3}$$

One of the key problems in the application of SVR model is to select an appropriate kernel function. Four kinds of kernel functions are commonly used, namely linear, polynomial, sigmoid and Gaussian (radial basis) (Çevik et al. 2015). Considering the efficiency and reliability, especially in the face of a variety of parameters, Gaussian kernel function is selected here as shown below:

$$K(x, x_i) = \exp\left(-\gamma \|x - x_i\|^2\right) \tag{4}$$

where  $\gamma$  is the kernel parameter. The generalization ability of SVR depends on the proper setting of parameters  $C, \gamma$  and  $\varepsilon$ . Genetic algorithm is used to determine the optimal value of parameters.

#### 4.2 Genetic algorithm (GA)

In the past few years, GA has been applied as an effective tool to solve different optimization problems in engineering and academia (Yan and Lin 2016; Chatterjee et al. 2017; Umeonyiagu and Nwobi-Okoye 2019). GA is not only a global optimization search algorithm by simulating the process of natural selection and biological evolution (Taylor 1994), but also a probabilistic parallel optimization method, which can adjust the search direction adaptively without the need of certain rules. The main characteristic is that it acts directly on the target object and uses the fitness function instead of the cost function without the requirement of function continuity and derivability. The complex problem can be solved by three genetic operations: selection, crossover and mutation.

In the GA, search parameters are binary encoded to produce many binary strings called chromosomes. Multiple chromosomes form an initial population. The aim is to get

Fig. 1 Typical geometry and cross section of a rectangular beam

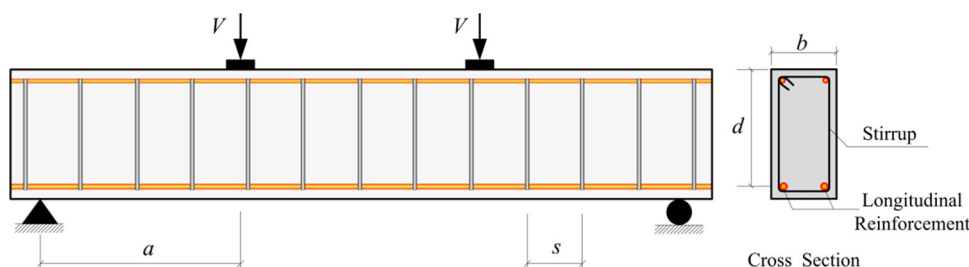


**Table 1** Initial statistical parameters for the experimental dataset

Parameter	$s$ (mm)	$b$ (mm)	$a/d$	$d$ (mm)	$f_c$ (MPa)	$f_t$ (MPa)	$\rho$ (%)	$\rho_{sv}f_{yv}$ (MPa)	$v_u$ (MPa)
Minimum	60.00	40.00	0.79	114.00	23.60	1.96	0.50	12.02	1.17
Mean	179.10	122.47	2.67	277.39	109.60	7.49	3.78	274.29	12.11
Maximum	1000.00	200.00	5.00	430.00	232.10	24.18	13.57	1045.00	31.08
Median	151.00	120.00	2.50	270.27	116.70	6.14	3.25	141.74	9.67
Std*	116.51	51.59	1.02	81.40	53.36	4.67	2.76	256.32	8.55
Cov*	0.65	0.42	0.38	0.29	0.49	0.62	0.73	0.93	0.71

\*Std and Cov denotes the standard deviation and the coefficient of variable, respectively. When there was no test value of tensile strength  $f_t$ , 0.75 times of splitting strength was taken (Zheng et al. 2019)

a qualified set of chromosomes after limited generations. For this purpose, a fitness function associated with chromosomes is defined. The higher fitness, the higher probability of chromosome selection, and then the selected chromosomes are crossed and mutated to produce a new population. Finally, a chromosome with the best fitness is obtained after finite generations, which is decoded to obtain optimal parameters. From this process, it can be seen that GA is independent of the specific domain of the problem and very robust to various optimization problems. The searching efficiency of GA is affected by some factors, such as population size, crossover probability and mutation probability, but it is out the scope of our paper.

### 4.3 The hybridized SVR-GA model

The main problem of SVR model is to select appropriate kernel function and hyper parameters, which is time consuming work (Çevik et al. 2015). GA can be employed to quickly select the optimal parameters for SVR model. The flow diagram of proposed hybrid SVR-GA model was shown in Fig. 2. In the SVR-GA model, the population size was 50, while the evolutionary iteration was 200 generations, and the probability of crossover and mutation was 0.8 and 0.09, respectively. The SVR parameters,  $C$  and  $\gamma$  were binary encoded while  $\varepsilon$  was always 0.01. For better evolution, the fitness function here adopts the correlation coefficient, which is calculated by the experimental value and predicted value of the SVR model. Higher fitness value means higher ranking for a chromosome, while a lower ranking chromosome is less likely to be selected. According to the principles of survival of the fittest, the latest generation chromosome with the best fitness can be decoded as the approximate optimal parameter after generation after generation of selection, crossover, and mutation. In the end, the optimal parameters can be obtained for the SVR model used for data training and model validation, and the well trained SVR-GA model for prediction with high accuracy can be obtained. The key parameters of SVR named  $C$  and  $\gamma$  can be determined by the pseudo-code combing GA (Deveci and Demirel 2018; Gao et al. 2019)

and SVR shown in Algorithm 1 with initial parameters shown in Table 2.

#### Algorithm 1. The hybrid SVR-GA

```

Input: Cmin; Cmax;  $\gamma$ min;  $\gamma$ max; population_size; max_generation;
probability_crossover; probability_mutation; DS_train; DS_validate;
DS_test. /*DS is the normal dataset of samples */
Output: C;  $\gamma$ ; DS_prediction; MSE
Begin
1 Len_chromosome = ceil(Cmin, Cmax,  $\gamma$ min,  $\gamma$ max); /* invoke ceil for
evaluate chromosome length /
2 Initialize population of chromosomes  $\leftarrow$  Len_chromosome and
population_size ;
3 C and  $\gamma \leftarrow$  the chromosomes; /* Decoding /
4 Model= SVMtrain(C,  $\gamma$ , DS_train); /* invoke svmtrain from libSVM-
3.23 for model training/
5 Evaluate the fitness MSE  $\leftarrow$  SVMpredict(DS_validate , Model )
6 For i =1 to max_generation
7 Choose the best chromosomes using Roulette Wheel;
/* The best chromosome corresponds to the smallest MSE /
8 Generate new chromosomes through crossover and mutation;
/*Using probability_crossover and probability_mutation /
9 C and  $\gamma \leftarrow$  the new chromosomes; /* Decoding /
10 Model = SVMtrain(C,  $\gamma$ , DS_train);
11 Evaluate the fitness MSE  $\leftarrow$  SVMpredict (DS_validate , Model )
12 Replacing the worst chromosomes of the population with the best;
13 End For
14 Get the best C and  $\gamma$ ;
15 Model = SVMtrain(C,  $\gamma$ , DS_train and DS_validate);
16 DS_prediction and MSE  $\leftarrow$  SVMpredict(DS_prediction , Model );
End

```

## 5 Model implementation and performance metrics

The dataset containing 148 experimental samples was split into training set and testing set for SVR-GA. 16% of the dataset (24 samples) were randomly selected as testing set, which were not involved in the model training. The remaining 84% of the dataset (124 samples) were used to

**Fig. 2** Flow diagram of hybrid SVR-GA model

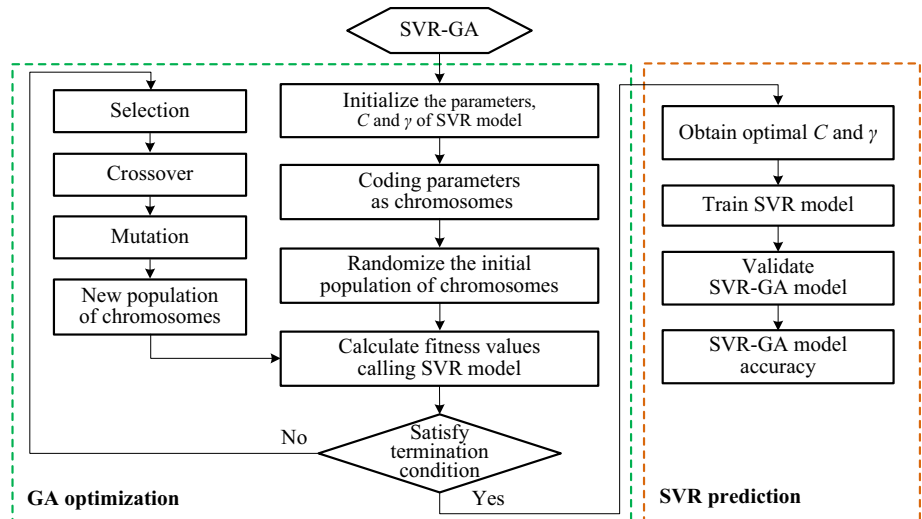


**Table 2** The initial parameters used in SVR-GA

Parameter	Value
Type	Real coded
Selection	Roulette wheel
Probability of crossover	0.8
Probability of mutation	0.09
Population size	50
Maximum number of generations	200
$(C_{min}, C_{max})$	$(2^{-10}, 2^{10})$
$(\gamma_{min}, \gamma_{max})$	$(2^{-10}, 2^{10})$

train and validate the model. To accurately evaluate the prediction ability of the model preventing from over-fitting and under-fitting conditions, a fivefold cross-validation method was utilized. It means the training set was divided into five equally sized subsets. Each fold was used to validate and obtain the optimal hyper-parameters (i.e.,  $C, \gamma$ ) for SVR model by GA, while the other fourfolds were used to train SVR model and get parameters  $w$  and  $b$ . In this process, one SVR-GA sub-model ( $f_i$ ) is generated for each fold. Over all folds, the average training error was calculated through five SVR-GA sub-model using all training set. The final prediction model of SVR-GA takes the average of the five sub-model predictions. More details for the fivefold cross-validation method in modeling process were shown in Fig. 3.

The experimental dataset was normalized with Eq. 5 before model training and testing, where  $x_n$  is the normalized value of experimental data ( $x_{real}$ ), between  $-1$  and  $1$ .  $x_{max}$  and  $x_{min}$  are the maximum and minimum values of  $x_{real}$ , respectively. After model predictions, the inverse

normalization is needed for the predicted data shown in Eq. 6.

$$x_n = 2 \frac{x_{real} - x_{min}}{x_{max} - x_{min}} - 1 \tag{5}$$

$$x_{real} = \frac{(x_n + 1)(x_{max} - x_{min})}{2} + x_{min} \tag{6}$$

Here, four statistical metrics are used to measure performance of proposed model, such as coefficient of determination ( $R^2$ ), mean absolute error (MAE), root mean squared error (RMSE), mean square error (MSE). The closer the value of  $R^2$  gets to 1, the better the prediction achieves. The formula of  $R^2$  can be shown as below.

$$R^2 = \frac{[\sum_{i=1}^n (y_i - \bar{y})(\hat{y}_i - \bar{\hat{y}})]^2}{\sum_{i=1}^n (y_i - \bar{y})^2 \sum_{i=1}^n (\hat{y}_i - \bar{\hat{y}})^2} \tag{7}$$

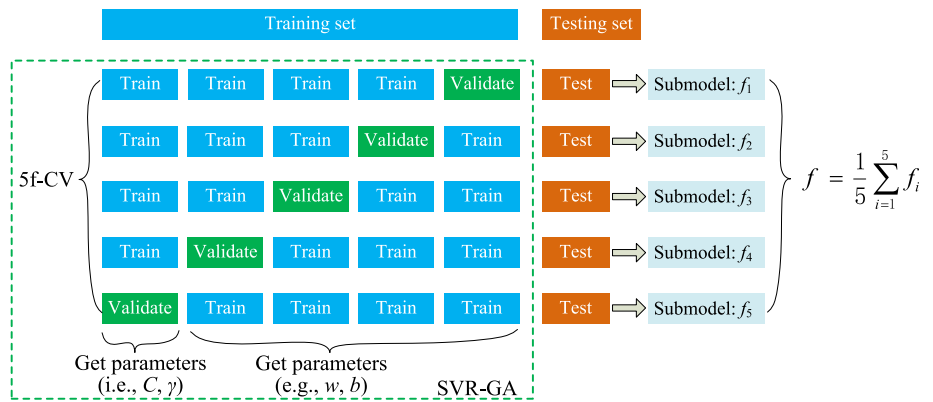
where  $y_i$  and  $\hat{y}_i$  are the  $i$ th observed and predicted values, respectively.  $\bar{y}$  and  $\bar{\hat{y}}$  are mean values of observed and predicted, respectively.  $n$  is the total number of observations. The low values of MAE and RMSE indicate good prediction accuracy of the model. MAE, MSE and RMSE are given by Eqs. 8–10.

$$MAE = \sum_{i=1}^n |y_i - \hat{y}_i| / n \tag{8}$$

$$MSE = \sum_{i=1}^n (y_i - \hat{y}_i)^2 / n \tag{9}$$

$$RMSE = \sqrt{\sum_{i=1}^n (y_i - \hat{y}_i)^2 / n} \tag{10}$$

**Fig. 3** Schematic diagram of the fivefold cross-validation and mean prediction model



### 6 Results and discussion

In this section, we employed three ML models including MLR, SVR and also SVR-GA to estimate the shear strength of medium- to ultra-high concrete strength beams with stirrups. The results of the three proposed models are compared with the results of the last edition of ACI 318.

Scatter plots with plumb error lines for the results of the proposed models based on training set are shown in Figs. 4, 5, 6 and 7. It is clear from Fig. 4 that SVR-GA has more accuracy than the other two ML models, as well as ACI 318. The box diagrams of the ratio of experimental value to predicted value for both training set and testing set are shown in Fig. 8. Compared to MLR and ACI 318, the upper and lower quartiles and the median of both two SVR and SVR-GA are all close to 1 with small dispersion, indicating that both SVR model and SVR-GA model can well predict the shear strength, and the SVR-GA model performs better than the SVR model for both training set and testing set. Furthermore, we also made comparison between experimental shear strength and predicted value of SVR-GA, SVR, MLR and ACI 318, the scatter plots are shown in Figs. 9 and 10 for the training set and testing set, respectively. It shows that all ML proposed models has better results than that for ACI 318 equations. A summary

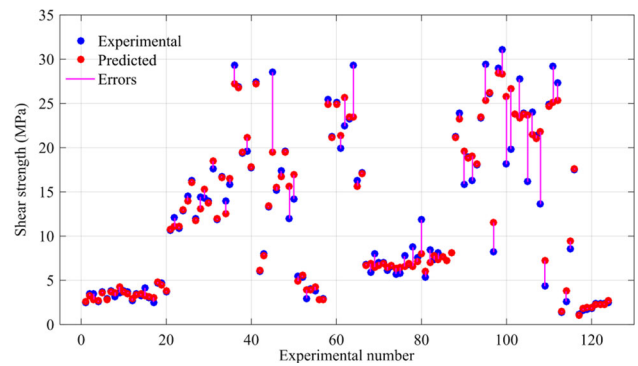


**Fig. 5** The comparison of experimental strength to predicted strength for SVR with training set

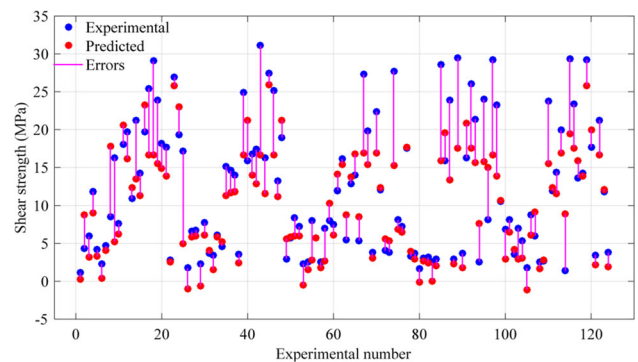


**Fig. 6** The comparison of experimental strength to predicted strength for MLR with training set

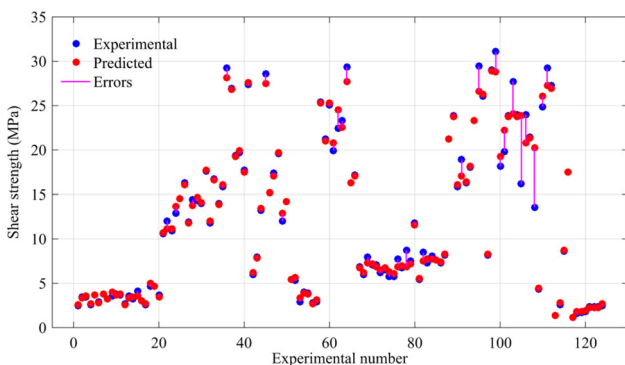


**Fig. 4** The comparison of experimental strength to predicted strength for SVR-GA with training set

result of the proposed models are also presented in Table 3, which reveals that SVR-GA achieves the least RMSE, the highest  $R^2$  and minimum MAE in both training set and testing set. Therefore, the SVR-GA model is a useful model for predicting the considered target.

According to the description above, SVR-GA had better results than other models, which is proposed for the considered prediction in this study. All figures indicated that the SVR-GA reflects the best performance, and further it had been applied for the sensitivity analysis to explore the

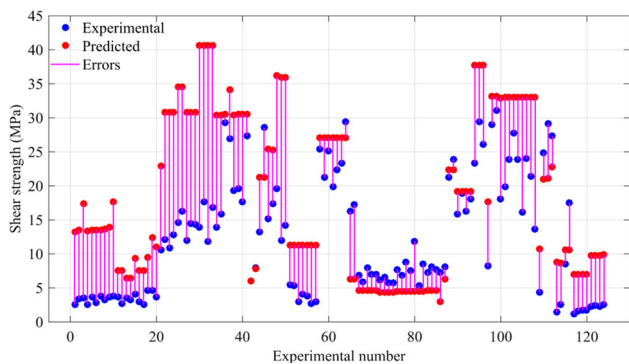


**Fig. 7** The comparison of experimental strength to predicted strength for ACI 318 with training set

importance of each input. More details of proposed models are shown in the following section.

### 6.1 Performance comparison of various models

Considering that MLR model is the most classical prediction model, it is also used as a comparison model. Performances of the MLR, SVR and SVR-GA are investigated and discussed based on the training set and testing set. Here, these models predict results are compared with ACI 318. The developed models were all applied to learn the relationship between the normalized ultimate shear strength ( $v_u$ ) and eight different input variables ( $s, b, h_0, f_c, f_t, \rho$  and  $\rho_{sv}f_{yv}$ ). In order to visualize the results of the models, the experimental and predicted shear strength values versus the experiment number of training set are presented graphically in scatter diagrams shown in Figs. 4, 5, 6 and 7 for the models of SVR-GA, SVR, MLR and ACI 318, respectively. Plumb lines are drawn to indicate prediction errors between the values of experimental shear strength and predicted shear strength. It can be seen that most of the predicted points are closest to the experimental points with SVR-GA model relative to the other models. It also reveals that the predicted errors in the SVR-GA model

are lowest following by SVR model. And the prediction result of ACI 318 is too conservative, and its prediction accuracy is worse than all three ML models above. Meanwhile, the predicted errors of SVR and MLR mainly appear in the region of high shear strength, and they also increase with the increase in shear strength. One possible reason is that there are fewer experimental data points available in this region compared to other regions.

The prediction error analysis box diagram of the ratio of experimental value to predicted value is shown graphically in Fig. 8. As a statistical diagram, the box diagram can provide key information about the location and dispersion of the data, and it can also clearly show the maximum, minimum, median, and upper and lower quartiles of the data. When the ratio of the predicted value to the test value is used as the input data of the box diagram, the closer the data point is to 1 and the lower the dispersion degree gets, the higher the accuracy the model can achieve. As seen in Fig. 8, compared to MLR and ACI 318, the upper and lower quartiles and the median of both two SVR and SVR-GA are close to 1 and the degree of dispersion is very small, especially for the SVR-GA model. It suggests that both SVR model and SVR-GA model can well predict the shear strength, and the SVR-GA model performs better than the SVR model.

The comparison of the experimental shear strength with the predicted value of the SVR-GA, SVR, MLR and ACI 318 is presented graphically in scatter plot shown in Figs. 9 and 10 for the training set and testing set, respectively. The fitting lines of the experimental and predicted value are also shown in the figures. It can be seen that the closer the fitting line is to the perfect line (the included angle with the  $x$ -axis is to  $45^\circ$ ), the better predicted performance the model works. The angle slope of the fitting line is close to the perfect line in both the training set and testing set for SVR-GA and SVR. This validates the consistency of the models of SVR-GA and SVR. We can also derive that the predicted values of the SVR-GA model have less

**Fig. 8** Comparison of the model error of MLR, SVR and SVR-GA model

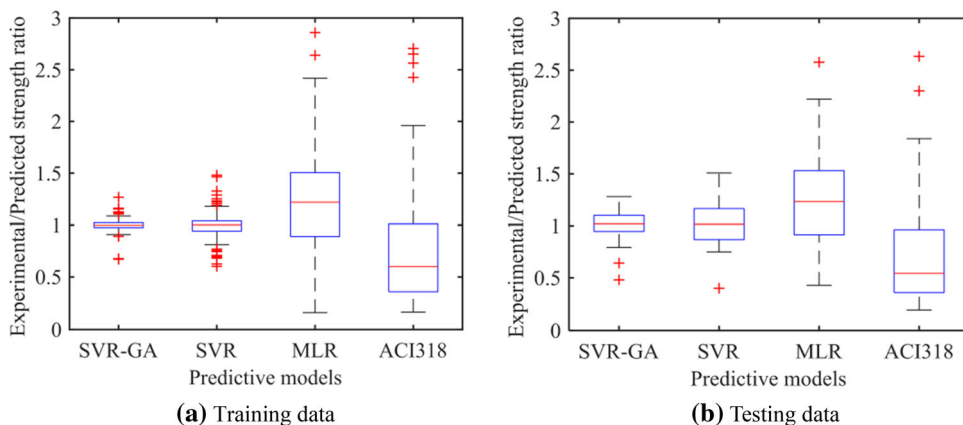
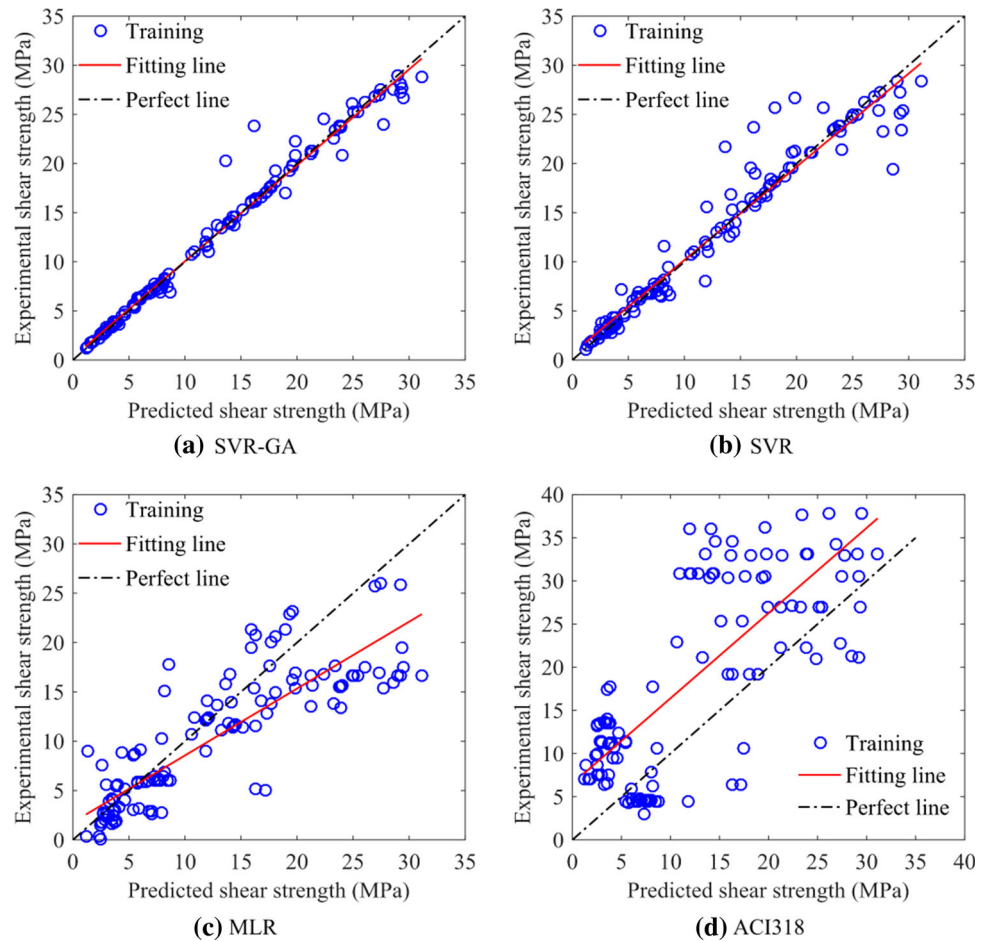




**Fig. 9** The comparison of experimental strength to predicted strength using the training data



dispersion compared with the SVR model based on both training set and the testing set indicating that the SVR-GA model surpasses the SVR model. As shown in Figs. 9d and 10d, the fitting line of ACI 318 is above and almost parallel to the perfect line, indicating that it is too conservative. The predicted values of ACI 318 are the most dispersed, followed by MLR.

To further determine the accuracies of the four models mentioned above, different metrics such as  $R^2$ , RMSE, MSE and MAE are measured by Eqs. 7–10. The reported statistical results are shown in Table 3 for both the training set and testing set. The SVR-GA model performs best both in the training stage and testing stage recorded with highest values of  $R^2$  and the lowest values of RMSE, MSE and MAE. To be specific, for the training set,  $R^2 = 0.9806$ , RMSE = 1.2055, MSE = 1.4533 and MAE = 0.5281. Contrast to SVR model with  $R^2 = 0.9419$ , RMSE = 2.0882, MSE = 4.3605 and MAE = 1.0773, MLR model with a lower  $R^2$  (0.7303), higher RMSE (5.0122), MSE (25.1217) and MAE (3.6367), while ACI 318 has the lowest  $R^2$  (0.5274), highest RMSE (10.2943), MSE (105.9724) and MAE (8.2110). Meanwhile, for the testing set, SVR-GA model with the highest  $R^2$  (0.9642), lowest

RMSE (1.4685), MSE (2.1566) and MAE (1.0216), following by SVR model with  $R^2$  (0.9379), higher RMSE (2.0375), MSE (4.1513) and MAE (1.4973). And there were the lower  $R^2$  (0.9642), higher RMSE (1.4685), MSE (2.1566) and MAE (1.0216) for MLR model, while there are the lowest  $R^2$  (0.5410), highest RMSE (11.1574), MSE (124.6848) and MAE (9.3290) for ACI 318. It reveals that the MAE and RMSE values of the SVR-GA model are lowest among other models in Fig. 11. These results show that the SVR-GA model can achieve best performance in ultimate shear strength prediction. More details can be seen in Table 3.

It can be derived from the above analysis that the highest precision prediction value can be obtained by using SVR-GA, while results obtained by ACI 318 are worse than all of ML models mentioned above both in training data and testing data. It also demonstrates that SVR-GA model can achieve best prediction effect on the shear strength of medium- to ultra-high-strength concrete beams, which is superior to the traditional SVR model, MLR model and ACI 318. Therefore, we applied SVR-GA model for sensitivity analysis in the following section.

**Fig. 10** The comparison of experimental strength to predicted strength using the testing data

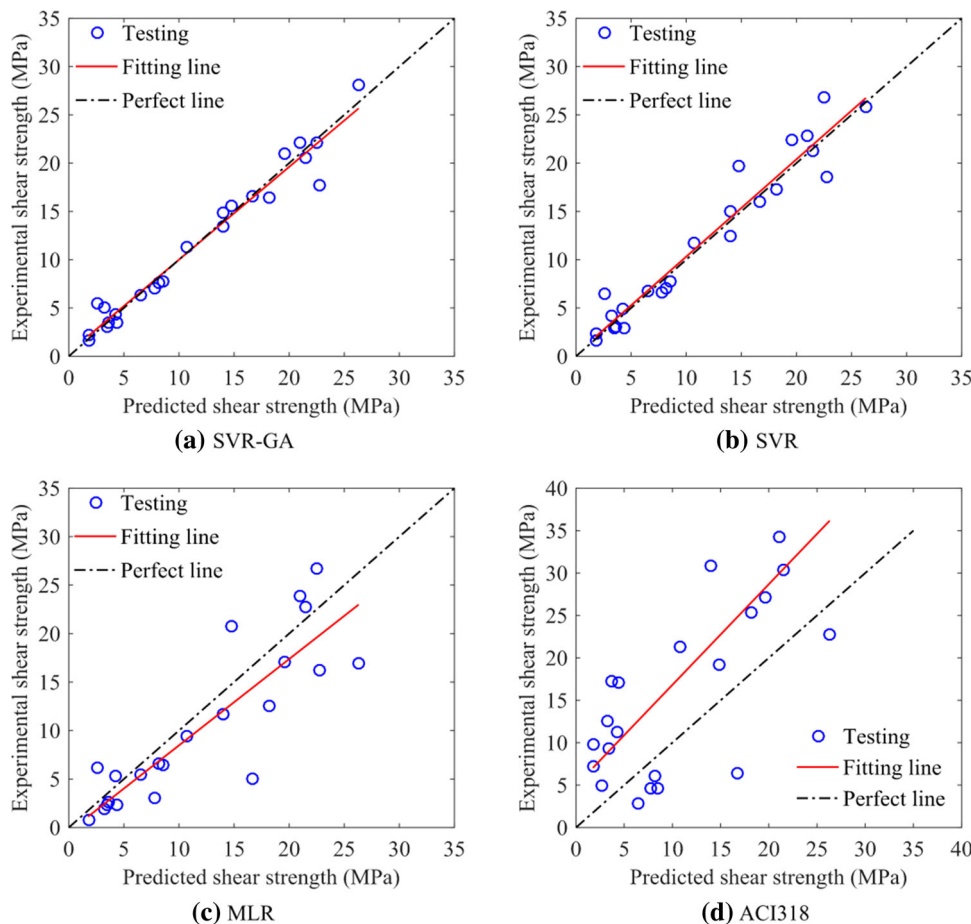


**Table 3** Statistical properties of the developed models

Parameters	SVR-GA model		SVR model		MLR model		ACI 318	
	Training data	Testing data	Training data	Testing data	Training data	Testing data	Training data	Testing data
$R^2$	0.9806	0.9642	0.9419	0.9379	0.7303	0.7667	0.5274	0.5410
RMSE	1.2055	1.4685	2.0882	2.0375	5.0122	4.2566	10.2943	11.1574
MSE	1.4533	2.1566	4.3605	4.1513	25.1217	18.1182	105.9724	124.6848
MAE	0.5281	1.0216	1.0773	1.4973	3.6367	3.2728	8.2110	9.3290
Mean*	0.9988	0.9999	0.9949	0.9995	1.3720	1.1609	0.7806	0.8041
Std*	0.0696	0.1745	0.1354	0.2181	3.5749	1.2823	0.5634	0.6754

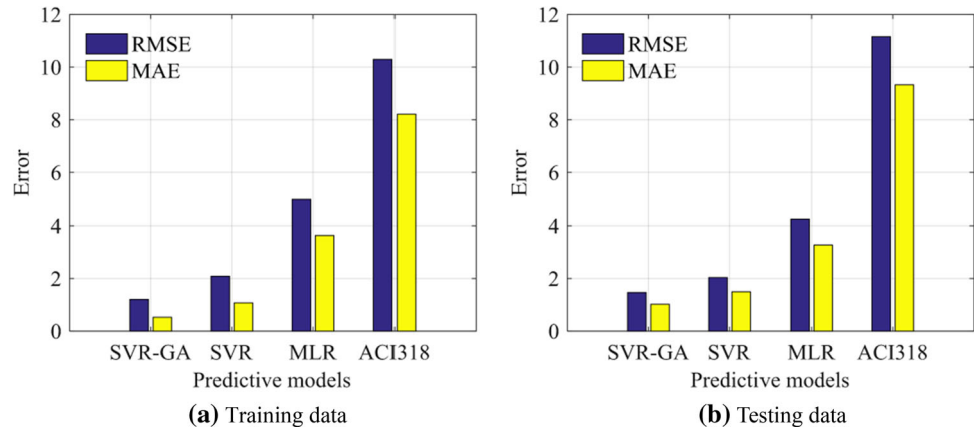
\*Mean and Std are respectively, the mean and standard deviation of the ratio of the experimental shear strength to the predicted value

### 6.2 Sensitivity analysis

The sensitivity analysis is implemented for exploring the important degree of each of the input variables using the SVR-GA model. Twentieth quantiles (from minimum to maximum, increased by 5%) of each input variable collated from the experimental dataset are used as a new dataset to calculate the normalized ultimate shear strength. To be more precise, the value of one input varies from minimum

to maximum, while all other inputs remain with their average values. According to the statistical probability distribution of input variables, the influence of input variable changes on output results is explored shown in Table 4. For example, the minimum value (0.79) and maximum value (5.0) of  $a/d$ , and the median value of other parameters are taken to predict the shear strength as  $v_{max}$  (15.7606 MPa) and  $v_{min}$  (4.9361 MPa), then the important degree of this variable is  $(v_{max} - v_{min})/v_{max} = 0.6868$ . The

**Fig. 11** Comparison of the RMSE and MAE of MLR, SVR and SVR-GA model



sensitivity analysis results for each input are presented graphically in bar chart shown in Fig. 12. The figure reveals that all input variables can affect the prediction of the shear strength through the SVR-GA model. The most important variables are  $a/d$ ,  $f_c$ ,  $\rho$  and  $\rho_{sv}f_{yv}$ , with the degree of importance values of 0.6868, 0.6044, 0.4615 and 0.4607, respectively. This information is highly relevant to the literature (Wang et al. 2020), and is consistent with the results of the literature that the most important parameters are the shear span-to-depth ratio and concrete compressive strength. However, Fig. 12 reveals that the stirrup spacing has little effect on the shear strength of the slender beam, and its important degree is only 0.1658. It is noteworthy that although the range of stirrup spacing in the experimental dataset is very large ranging from 20 to 1000 mm, the median value is only 151 mm, and most of the data are small. Consequently, a larger database of larger stirrup spacing should be considered in future research to explore the degree of importance of the stirrup spacing.

The sensitivity analysis described above shows that machine learning and artificial intelligence technologies can be helpful during the design of beam shear resistance phase. In addition to accurately predicting the ultimate shear strength, the SVR-GA model can also help create more informative input/output maps of the ultimate shear strength. Especially, the most important variables ( $a/d$ ,  $f_c$ ,  $\rho$  and  $\rho_{sv}f_{yv}$ ) will be used here to illustrate the input and output maps of the ultimate shear strength. The values of the other variables remain the same as the average value. Six ultimate shear strength maps with the same color range are presented in Fig. 13, which shows the relationship diagrams of  $f_c$  and  $a/d$ ,  $f_c$  and  $\rho_{sv}f_{yv}$ ,  $f_c$  and  $\rho$ ,  $a/d$  and  $\rho_{sv}f_{yv}$ ,  $a/d$  and  $\rho$ ,  $\rho$  and  $\rho_{sv}f_{yv}$ , respectively. Three-dimensional maps indicate that there is a nonlinear behavior in the input and output relationship, which makes it difficult to detect their relationship only from the experimental data. Except that the increase in  $a/d$  will reduce the shear strength to some extent, the increase in other input variables will

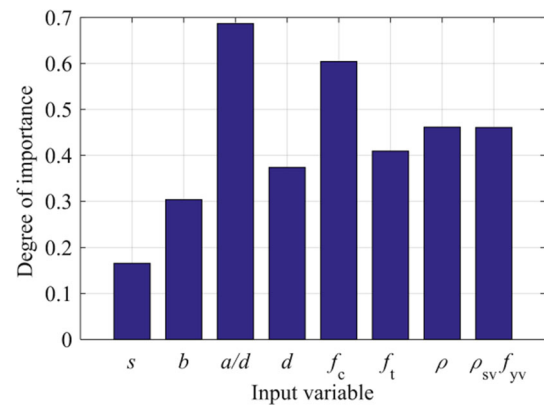


**Fig. 12** Bar chart of the degree of importance value estimation

increase the shear strength to varying degrees. Figure 13a and f shows an interesting phenomenon that the ultimate shear strength is not the maximum, when the two most important factors ( $a/d$  and  $f_c$ ) are both used as inputs. On the contrary, the ultimate shear strength reaches the maximum, when taking the two lower important factors ( $\rho$  and  $\rho_{sv}f_{yv}$ ) as inputs. This reflects from the side that the shear strength calculation of the beam with stirrups is extremely complex, which is the result of the coupling of multiple variables, and the variables cannot be considered separately.

It can be derived from the above analysis that the highest precision prediction value can be obtained by using SVR-GA while results obtained by ACI 318 are worse than all of ML models mentioned above both in training data and testing data. It also demonstrates that SVR-GA model can achieve best prediction effect on the shear strength of medium- to ultra-high-strength concrete beams, which is superior to the traditional SVR model, MLR model and ACI 318.

**Table 4** Values of the variables used to calculate the degree of importance

$s$ (mm)	$b$ (mm)	$a/d$	$d$ (mm)	$f_c$ (MPa)	$f_t$ (MPa)	$\rho$ (%)	$\rho_{sv}f_{yv}$ (MPa)	$v_u$ (MPa)	DI*
<b>1000</b>	122.47	2.67	277.4	109.6	7.49	3.78	274.29	15.1803	0.1658
<b>60</b>	122.47	2.67	277.4	109.6	7.49	3.78	274.29	12.6631	
179.1	<b>200</b>	2.67	277.4	109.6	7.49	3.78	274.29	11.5489	0.3036
179.1	<b>40</b>	2.67	277.4	109.6	7.49	3.78	274.29	16.5844	
179.1	122.47	<b>5.00</b>	277.4	109.6	7.49	3.78	274.29	<b>4.9361</b>	<b>0.6868</b>
179.1	122.47	<b>0.79</b>	277.4	109.6	7.49	3.78	274.29	<b>15.7606</b>	
179.1	122.47	2.67	<b>430</b>	109.6	7.49	3.78	274.29	7.1733	0.3738
179.1	122.47	2.67	<b>114</b>	109.6	7.49	3.78	274.29	11.4559	
179.1	122.47	2.67	277.4	<b>232.1</b>	7.49	3.78	274.29	23.7992	0.6044
179.1	122.47	2.67	277.4	<b>23.6</b>	7.49	3.78	274.29	9.4155	
179.1	122.47	2.67	277.4	109.6	<b>24.18</b>	3.78	274.29	16.2389	0.4094
179.1	122.47	2.67	277.4	109.6	<b>1.96</b>	3.78	274.29	9.5910	
179.1	122.47	2.67	277.4	109.6	7.49	<b>13.57</b>	274.29	18.3481	0.4615
179.1	122.47	2.67	277.4	109.6	7.49	<b>0.5</b>	274.29	9.8808	
179.1	122.47	2.67	277.4	109.6	7.49	3.78	<b>1045</b>	20.0627	0.4607
179.1	122.47	2.67	277.4	109.6	7.49	3.78	<b>12.02</b>	10.8193	

Bold font indicates the maximum value and minimum value of the input variables. While the values of  $v_u$  in bold font are used to show the predicted shear strength of the input variable  $a/d$  with minimum value (0.79) and maximum value (5.0), respectively, and the degree of importance (DI\*) of  $a/d$  is equal to 0.6868 in bold font calculated by  $(v_{\max}-v_{\min})/v_{\max}$

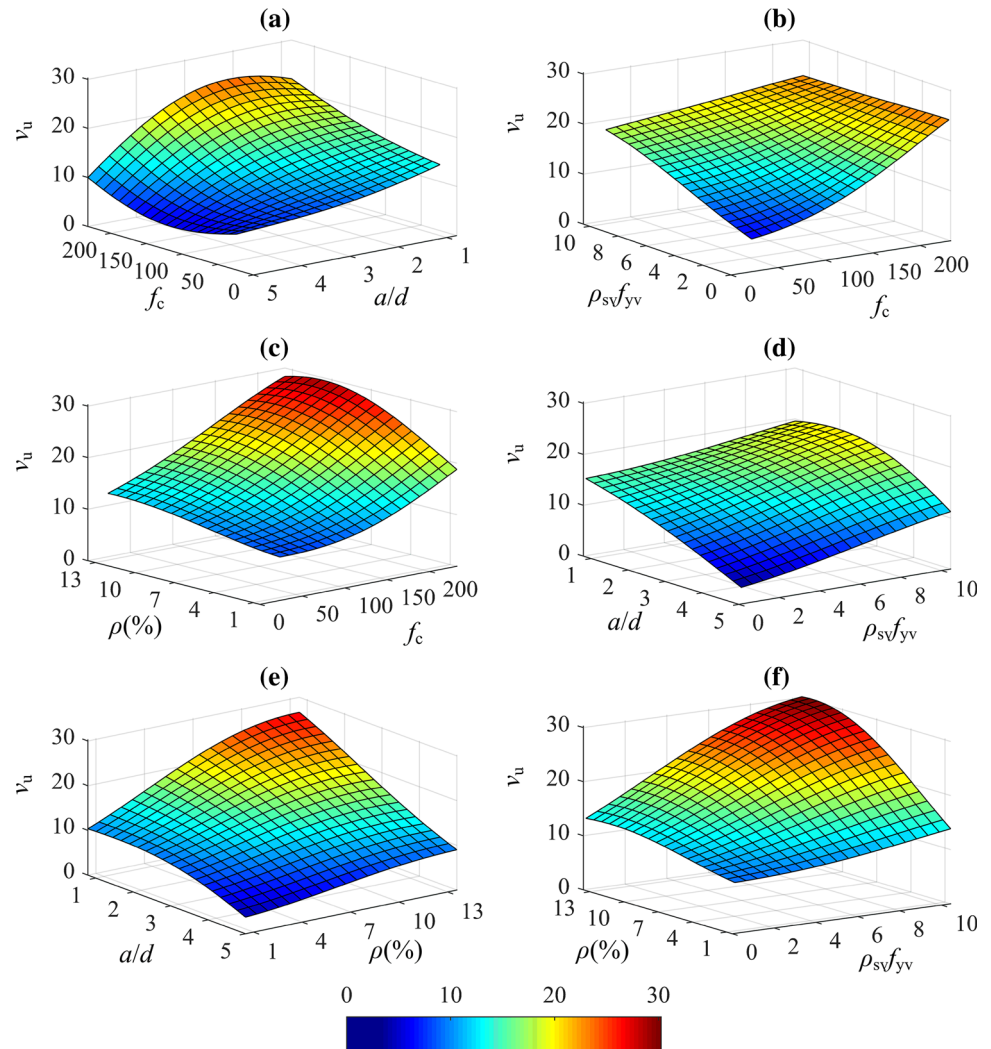
\*DI denotes the degree of importance

## 7 Conclusions

In this study, machine learning models for prediction goals is investigated to propose an effective model with high accuracy to calculate the shear strength of medium- to ultra-high concrete strength beams with stirrups. For this purpose, three ML models including MLR, SVR and SVR-GA are considered and discussed. All models are trained and tested based on an experimental database with 148 samples gathered from literatures, which consists of eight input variables including stirrup spacing, beam width, shear span-to-depth ratio, effective depth of the beam, concrete compressive strength, concrete tensile strength, longitudinal reinforcement ratio and the product of the stirrup ratio and the stirrup yield strength. These inputs are applied in order to determine the shear strength of the considered medium- to ultra-high concrete beams with stirrups. The performances of the proposed ML models are compared with each other and also with ACI 318. The experimental results indicated that all ML models under fivefold cross-validation can achieve lower errors than ACI 318 equations, and the SVR model with optimal parameters obtained by GA had best performance than the other models, which can be applied to predict the shear strength.

It is also concluded that SVR-GA can be used as a suitable tool to predict the shear strength of ultra-high concrete beams with stirrups with a high level of precision. Furthermore, the sensitivity analysis reveals that all input variables can affect the prediction accuracy of the shear strength, and the most important variables are shear span-to-depth ratio, concrete compressive strength, longitudinal reinforcement ratio and the product of the stirrup ratio and the stirrup yield strength. The proposed SVR-GA model here can be a guide with high prediction accuracy for the shear strength design of ultra-high concrete beams with stirrups. It is expected that the shear strength of medium- to ultra-high strength concrete beams with any combination of design parameters can be predicted accurately providing guides for optimal design. At the same time, there are still some issues that need to be resolved. For example, there is poor interpretability for the proposed SVR-GA model, making it difficult to be well understood by designers for optimal design of medium- to ultra-high strength concrete beams with stirrups. The future works can be done with more experimental data with other more interpretable models.

**Fig. 13** Three-dimensional input and output maps of the ultimate shear strength: **a**  $f_c$ - $a/d$ , **b**  $f_c$ - $\rho_{sv}f_{yv}$ , **c**  $f_c$ - $\rho$ , **d**  $a/d$ - $\rho_{sv}f_{yv}$ , **e**  $a/d$ - $\rho$ , and **f**  $\rho$ - $\rho_{sv}f_{yv}$



**Funding** The authors are very grateful for the support of the Guangxi Basic Ability Promotion Project for Young and Middle-aged Teachers (No. 2018KY0241). At the same time, we would also like to thank the distinguished reviewers and editors for their excellent suggestions and comments.

## Declarations

**Conflict of interest** The authors declare no conflict of interest.

**Human and animal rights** This article does not include any studies of human participants performed by the authors.

**Credit authorship contribution statement** C-SJ: Conceptualization, Methodology, Formal analysis, Writing & editing. G-QL: Supervision, Resources, Review & editing.

## References

ACI Committee 318 (2014) *Acı 318-14*

- Açıkgenç M, Ulaş M, Alyamaç KE (2015) Using an artificial neural network to predict mix compositions of steel fiber-reinforced concrete. *Arab J Sci Eng* 40(2):407–419. <https://doi.org/10.1007/s13369-014-1549-x>
- Baby F, Marchand P, Toutlemonde F (2014) Shear behavior of ultrahigh performance fiber-reinforced concrete beams. I: experimental investigation. *J Struct Eng* 140(5):04013111. [https://doi.org/10.1061/\(asce\)st.1943-541x.0000907](https://doi.org/10.1061/(asce)st.1943-541x.0000907)
- Ccoicca YJ (2013) Applications of support vector machines in the exploratory phase of petroleum and natural gas: a Survey. *Int J Eng Technol* 2(2):113–125. <https://doi.org/10.14419/ijet.v2i2.834>
- Çevik A, Kurtoğlu AE, Bilgehan M et al (2015) Support vector machines in structural engineering: a review. *J Civ Eng Manag* 21(3):261–281. <https://doi.org/10.3846/13923730.2015.1005021>
- Chatterjee S, Sarkar S, Hore S et al (2017) Structural failure classification for reinforced concrete buildings using trained neural network based multi-objective genetic algorithm. *Struct Eng Mech*. <https://doi.org/10.12989/sem.2017.63.4.429>
- Collins MP, Bentz EC, Sherwood EG, Wight JK (2008) Where is shear reinforcement required? Review of research results and design procedures. *ACI Struct J* 105(5):590–600
- Demirel NÇ, Deveci M (2017) Novel search space updating heuristics-based genetic algorithm for optimizing medium-scale

- airline crew pairing problems. *Int J Comput Intell Syst* 10(1):1082–1101. <https://doi.org/10.2991/ijcis.2017.10.1.72>
- Deveci M, Demirel NC (2016) A hybrid genetic algorithm for airline crew pairing optimization. In: *Economic and social development: book of proceedings*. Zagreb, pp 118–124
- Deveci M, Demirel NÇ (2018) Evolutionary algorithms for solving the airline crew pairing problem. *Comput Ind Eng* 115:389–406. <https://doi.org/10.1016/j.cie.2017.11.022>
- Farfani HA, Behnamfar F, Fathollahi A (2015) Dynamic analysis of soil-structure interaction using the neural networks and the support vector machines. *Exp Syst Appl* 42(22):8971–8981. <https://doi.org/10.1016/j.eswa.2015.07.053>
- Gao S, Zhou M, Wang Y et al (2019) Dendritic neuron model with effective learning algorithms for classification, approximation, and prediction. *IEEE Trans Neural Netw Learn Syst* 30(2):1–14. <https://doi.org/10.1109/TNNLS.2018.2846646>
- Golafshani EM, Rahai A, Sebt MH (2015) Artificial neural network and genetic programming for predicting the bond strength of GFRP bars in concrete. *Mater Struct Constr* 48(5):1581–1602. <https://doi.org/10.1617/s11527-014-0256-0>
- Guo M, Hesthaven JS (2018) Reduced order modeling for nonlinear structural analysis using Gaussian process regression. *Comput Methods Appl Mech Eng* 341(1):807–826. <https://doi.org/10.1016/j.cma.2018.07.017>
- Hasgul U, Yavas A, Birol T, Turker K (2019) Steel fiber use as shear reinforcement on I-shaped UHP-FRC beams. *Appl Sci* 9(24):5526. <https://doi.org/10.3390/app9245526>
- Hassan AMT, Jones SW, Mahmud GH (2012) Experimental test methods to determine the uniaxial tensile and compressive behaviour of Ultra High Performance Fibre Reinforced Concrete(UHPFRC). *Constr Build Mater* 37(1):874–882. <https://doi.org/10.1016/j.conbuildmat.2012.04.030>
- Hoang ND, Pham AD, Nguyen QL, Pham QN (2016) Estimating compressive strength of high performance concrete with Gaussian process regression model. *Adv Civ Eng* 2016:2861380. <https://doi.org/10.1155/2016/2861380>
- Hossain KMA, Gladson LR, Anwar MS (2017) Modeling shear strength of medium- to ultra-high-strength steel fiber-reinforced concrete beams using artificial neural network. *Neural Comput Appl* 28(S1):S1119–S1130. <https://doi.org/10.1007/s00521-016-2417-2>
- Hou LJ, Luan ZY, Chen D, Xu SL (2015) Experimental study of the shear properties of reinforced ultra-high toughness cementitious composite beams. *J Zhejiang Univ Sci A* 16(4):251–264. <https://doi.org/10.1631/jzus.A1400274>
- Ji W, Ding B, An M (2011) Experimental study on the shear capacity of reactive powder concrete T-beams. *Zhongguo Tiedao Kexue/china Railw Sci* 32(5):38–42. <https://doi.org/10.1080/0144929X.2011.553739>
- Jin LZ, Li YX, Qi KN, He P (2015) Research on shear bearing capacity and ductility of high strength reinforced RPC beam. *Gongcheng Lixue/eng Mech* 32(1):209–214. <https://doi.org/10.6052/j.issn.1000-4750.2014.04.S056>
- Kamal MM, Safan MA, Etman ZA, Salama RA (2014) Behavior and strength of beams cast with ultra high strength concrete containing different types of fibers. *HBRC J* 10(1):55–63. <https://doi.org/10.1016/j.hbrj.2013.09.008>
- Krassowska J, Kosior-Kazberuk M, Berkowski P (2019) Shear behavior of two-span fiber reinforced concrete beams. *Arch Civ Mech Eng* 19(4):1442–1457. <https://doi.org/10.1016/j.acme.2019.09.005>
- Lim WY, Hong SG (2016) Shear tests for ultra-high performance fiber reinforced concrete (UHPFRC) beams with shear reinforcement. *Int J Concr Struct Mater* 10(2):177–188. <https://doi.org/10.1007/s40069-016-0145-8>
- Liu W, Wang Z, Liu X et al (2017) A survey of deep neural network architectures and their applications. *Neurocomputing* 234:1–31. <https://doi.org/10.1016/j.neucom.2016.12.038>
- Luo X, Zhou M, Li S, Shang M (2018a) An inherently nonnegative latent factor model for high-dimensional and sparse matrices from industrial applications. *IEEE Trans Ind Inform* 14(5):2011–2022. <https://doi.org/10.1109/TII.2017.2766528>
- Luo X, Zhou MC, Li S et al (2018b) Incorporation of efficient second-order solvers into latent factor models for accurate prediction of missing QoS data. *IEEE Trans Cybern* 48(4):1216–1228. <https://doi.org/10.1109/TCYB.2017.2685521>
- Luo X, Zhou MC, Xia Y et al (2016) Generating highly accurate predictions for missing QoS data via aggregating nonnegative latent factor models. *IEEE Trans Neural Netw Learn Syst* 27(3):524–537. <https://doi.org/10.1109/TNNLS.2015.2412037>
- Luo X, Qin W, Dong A et al (2021) Efficient and high-quality recommendations via momentum-incorporated parallel stochastic gradient descent-based learning. *IEEE/CAA J Autom Sin* 8(2):402–411. <https://doi.org/10.1109/JAS.2020.1003396>
- Magureanu C, Sosa I, Negrutiu C, Heghes B (2010) Bending and shear behavior of ultra-high performance fiber reinforced concrete. In: *WIT transactions on the built environment*, pp 79–89
- Mansouri I, Ozbakkaloglu T, Kisi O, Xie T (2016) Predicting behavior of FRP-confined concrete using neuro fuzzy, neural network, multivariate adaptive regression splines and M5 model tree techniques. *Mater Struct Constr* 49(10):4319–4334. <https://doi.org/10.1617/s11527-015-0790-4>
- Mari Bernat A, Spinella N, Recupero A, Cladera A (2020) Mechanical model for the shear strength of steel fiber reinforced concrete (SFRC) beams without stirrups. *Mater Struct Constr* 53(2):1–20. <https://doi.org/10.1617/s11527-020-01461-4>
- Mészöly T, Randl N (2018) Shear behavior of fiber-reinforced ultra-high performance concrete beams. *Eng Struct* 168:119–127. <https://doi.org/10.1016/j.engstruct.2018.04.075>
- Ministry of Transport of China (2018) Specifications for design of highway reinforced concrete and prestressed concrete bridges and culverts JTG 3362–2018. People’s Communications Press, Beijing
- Nguyen QH, Ly HB, Le TT et al (2020) Parametric investigation of particle swarm optimization to improve the performance of the adaptive neuro-fuzzy inference system in determining the buckling capacity of circular opening steel beams. *Materials (base)* 13:2210. <https://doi.org/10.3390/ma13102210>
- Olalusi OB, Viljoen C (2020) Model uncertainties and bias in SHEAR strength predictions of slender stirrup reinforced concrete beams. *Struct Concr* 21:316–332. <https://doi.org/10.1002/suco.201800273>
- Pal M, Deswal S (2011) Support vector regression based shear strength modelling of deep beams. *Comput Struct* 89:1430–1439. <https://doi.org/10.1016/j.compstruc.2011.03.005>
- Pansuk W, Nguyen TN, Sato Y et al (2017) Shear capacity of high performance fiber reinforced concrete I-beams. *Constr Build Mater* 157:182–193. <https://doi.org/10.1016/j.conbuildmat.2017.09.057>
- Press CSI (2010) Code for design of concrete structures GB 50010-2010. China Struct. Sci. Acad. Beijing
- Qi JN, Wang JQ, Zhou K et al (2020) Experimental and Theoretical Investigations on Shear Strength of UHPC Beams. *Zhongguo Gonglu Xuebao/china J Highw Transp* 33(7):95–103. <https://doi.org/10.19721/j.cnki.1001-7372.2020.07.010>
- Russo G, Somma G, Angeli P (2004) Design shear strength formula for high strength concrete beams. *Mater Struct Constr* 37:680–688. <https://doi.org/10.1617/14016>

- Sagaseta J, Vollum RL (2011) Influence of beam cross-section, loading arrangement and aggregate type on shear strength. *Mag Concr Res* 63(2):139–155. <https://doi.org/10.1680/mac.9.00192>
- Słowik M (2014) Shear failure mechanism in concrete beams. *Procedia Mater Sci* 3:1977–1982. <https://doi.org/10.1016/j.mspro.2014.06.318>
- Smarzewski P (2018) Hybrid fibres as shear reinforcement in high-performance concrete beams with and without openings. *Appl Sci* 8:2070. <https://doi.org/10.3390/app8112070>
- Solhmirzaei R, Salehi H, Kodur V, Naser MZ (2020) Machine learning framework for predicting failure mode and shear capacity of ultra high performance concrete beams. *Eng Struct* 224:111221. <https://doi.org/10.1016/j.engstruct.2020.111221>
- Taylor CE (1994) Adaptation in natural and artificial systems: an introductory analysis with applications to biology, control, and artificial intelligence. *Complex adaptive systems*. John H. Holland. *Q Rev Biol* 69. <https://doi.org/10.1086/418447>
- Teng S, Wu N, Zhu H et al (2018) SVM-DT-based adaptive and collaborative intrusion detection. *IEEE/CAA J Autom Sin* 5(1):108–118. <https://doi.org/10.1109/JAS.2017.7510730>
- Umeonyiagu IE, Nwobi-Okoye CC (2019) Modelling and multi objective optimization of bamboo reinforced concrete beams using ANN and genetic algorithms. *Eur J Wood Wood Prod* 77:931–947. <https://doi.org/10.1007/s00107-019-01418-7>
- Vapnik V, Golowich SE, Smola A (1997) Support vector method for function approximation, regression estimation, and signal processing. In: *Advances in neural information processing systems*
- Wang Q, Song HL, Lu CL, Jin LZ (2020) Shear performance of reinforced ultra-high performance concrete rectangular section beams. *Structures* 27(8):1184–1194. <https://doi.org/10.1016/j.istruc.2020.07.036>
- Xu H, Deng Z, Chen C, Chen X (2014) Experimental study on shear strength of ultra-high performance fiber reinforced concrete beams. *Tumu Gongcheng Xuebao/china Civ Eng J* 47(12):91–97
- Yan F, Lin Z (2016) New strategy for anchorage reliability assessment of GFRP bars to concrete using hybrid artificial neural network with genetic algorithm. *Compos Part B Eng* 92:420–433. <https://doi.org/10.1016/j.compositesb.2016.02.008>
- Yoo DY, Yoon YS (2016) A review on structural behavior, design, and application of ultra-high-performance fiber-reinforced concrete. *Int J Concr Struct Mater* 10(2):125–142. <https://doi.org/10.1007/s40069-016-0143-x>
- Yousef AM, Tahwia AM, Marami NA (2018) Minimum shear reinforcement for ultra-high performance fiber reinforced concrete deep beams. *Constr Build Mater* 184:177–185. <https://doi.org/10.1016/j.conbuildmat.2018.06.022>
- Yu PS, Chen ST, Chang IF (2006) Support vector regression for real-time flood stage forecasting. *J Hydrol* 328:704–716. <https://doi.org/10.1016/j.jhydrol.2006.01.021>
- Zhang HZ (2005) Experimental study on shear performance of high strength concrete beams. Dalian University of Technology, Dalian
- Zhang P, Shu S, Zhou M (2018) An online fault detection model and strategies based on SVM-grid in clouds. *IEEE/CAA J Autom Sin* 5(2):445–456. <https://doi.org/10.1109/JAS.2017.7510817>
- Zhang G, Ali ZH, Aldlemy MS et al (2020) Reinforced concrete deep beam shear strength capacity modelling using an integrative bio-inspired algorithm with an artificial intelligence model. *Eng Comput*. <https://doi.org/10.1007/s00366-020-01137-1>
- Zheng H, Fang Z, Chen B (2019) Experimental study on shear behavior of prestressed reactive powder concrete I-girders. *Front Struct Civ Eng* 13(3):618–627. <https://doi.org/10.1007/s11709-018-0500-8>
- Zhou JM, Chen S (2015) Experimental study and evaluation of the mechanical properties of reinforced concrete structures with high strength. Science Press, Beijing

**Publisher's Note** Springer Nature remains neutral with regard to jurisdictional claims in published maps and institutional affiliations.